The final publication is available at

https://doi.org/10.1002/hbm.23970

Additional Information

Regional hippocampal vulnerability in early multiple sclerosis: dynamic pathological spreading from dentate gyrus to CA1

Vincent Planche[1,2,3], Ismail Koubiyr[1,2], José E. Romero[4], José V. Manjon[4], Pierrick Coupé[5], Mathilde Deloire[3], Vincent Dousset[1,2,3], Bruno Brochet[1,2,3] , Aurélie Ruet[1,2,3,#] and Thomas Tourdias[1,2,3,#]

[1] Univ. Bordeaux, F-33000 Bordeaux, France

[2] Inserm U1215 - Neurocentre Magendie, F-33000 Bordeaux, France

[3] CHU de Bordeaux, F-33000 Bordeaux, France

[4] Instituto Universitario de Tecnologías de la Información y Comunicaciones (ITACA), Universitat Politècnica de València, Camino de Vera s/n, 46022 Valencia, España

[5] Laboratoire Bordelais de Recherche en Informatique, UMR CNRS 5800, PICTURA, F-33405 Talence, France

# Both authors contributed equally to this work

Corresponding author: Vincent Planche, Neurocentre Magendie, Inserm U1215, 146 Rue Léo Saignat, 33000, Bordeaux, France; planche.vincent@gmail.com; Phone: +33 (0)5 57 57 37 37; Fax: +33 (0)5 57 57 36 69

Short title: Hippocampal subfields vulnerability in MS

Key words: multiple sclerosis, clinically isolated syndrome, MRI, hippocampus, hippocampal subfields, dentate gyrus, CA1, memory impairment

Word count: abstract: 235, article: 4217 (with references)

Tables/Figures: 3 tables, 3 figures; 1 supplementary figure

References: 44

Abstract

Background: Whether hippocampal subfields are differentially vulnerable at the earliest stages of multiple sclerosis (MS) and how this impacts memory performance is a current topic of debate.

Methods: We prospectively included 56 persons with clinically isolated syndrome (CIS) suggestive of MS in a 1-year longitudinal study, together with 55 matched healthy controls at baseline. Participants were tested for memory performance and scanned with 3T MRI to assess the volume of 5 distinct hippocampal subfields using automatic segmentation techniques.

Results: At baseline, CA4/dentate gyrus was the only hippocampal subfield with a volume significantly smaller than controls ($p<0.01$). After one year, CA4/dentate gyrus atrophy worsened (-6.4%, $p<0.0001$) and significant CA1 atrophy appeared (both in the stratum-pyramidale and the stratum radiatum-lacunosum-moleculare, -5.6%, $p<0.001$ and -6.2%, $p<0.01$) respectively. CA4/dentate gyrus volume at baseline predicted CA1 volume one year after CIS ($R^2=0.44$ to 0.47, $p<0.001$, with age, T2 lesion-load and global brain atrophy as covariates). The volume of CA4/dentate gyrus at baseline was associated with MS diagnosis during follow-up, independently of T2-lesion load and demographic variables ($p<0.05$). Whereas CA4/dentate gyrus volume was not correlated with memory scores at baseline, CA1 atrophy was an independent correlate of episodic verbal memory performance one year after CIS (ß=0.87, $p<0.05$).

Conclusion: The hippocampal degenerative process spread from dentate gyrus to CA1 at the earliest stage of MS. This dynamic vulnerability is associated with MS diagnosis after CIS and will ultimately impact hippocampal-dependant memory performance.

Introduction

Patients with multiple sclerosis (MS) are often afflicted with episodic memory impairment and, over the past decade, a growing number of studies have investigated how hippocampal abnormalities might be related to this deficit [Sicotte et al., 2008; Dutta et al., 2011; Hulst et al., 2015; Planche et al., 2017a]. Post-mortem anatomopathological analyses of MS brains, together with studies on animal models of MS, have described early microglial activation, neuronal loss, synaptic dysfunction and demyelination within different regions of the hippocampus [Dutta et al., 2011; Papadopoulos et al., 2009; Planche et al., 2017b]. However, the time course of these alterations and the inter-relations between the different types of cellular modifications during the evolution of the disease remain largely unknown.

One way to isolate pathogenic mechanisms within the hippocampal circuit is to study its regional vulnerability [Small, 2014]. Indeed, the hippocampus is composed of distinct subfields whose morphological, cellular, molecular, functional and connectivity profiles are very different: the dentate gyrus, the cornu ammonis (CA, with subdivisions from CA1 to CA4) and the subiculum. Initially used to study Alzheimer's disease and physiological aging [West et al., 1994], this approach of interrogating differentially the malfunctioning hippocampal circuit has been adapted more recently to investigate MS [Sicotte et al., 2008; Gold et al., 2010; Longoni et al., 2015; Rocca et al., 2015].

Regarding MRI studies, the differential vulnerability of one hippocampal subfield compared to the others during the course of MS remains controversial. Indeed, some authors have highlighted the differential vulnerability of CA1 [Sicotte et al., 2008; Longoni et al., 2015] and others the vulnerability of CA3/CA4/dentate gyrus [Gold et al., 2010; Rocca et al., 2015]. The reasons for discrepancies between studies remain speculative but they might be explained

by the heterogeneity of the measurement methods used (surface-based mesh modelling and volumetric analyses) and/or by the heterogeneity of the populations studied (relapsing MS with different disease durations and/or progressive MS). This latter point seems crucial if we postulate that the pattern of atrophy of hippocampal subfields changes according to disease progression. Previous studies have so far been unable to test such timing and the dynamics of differential hippocampal subfield damage because of cross-sectional design. It is also important to note that none of these works investigated clinically isolated syndrome (CIS), which is required to address the question of the differential vulnerability of hippocampal subfields to the earliest pathophysiological mechanisms in MS. Indeed, CIS is the first demyelinating event suggestive of a future relapsing-remitting MS, that will be formally defined later on by the dissemination in time and space of demyelinating lesions [Polman et al., 2011; Miller et al., 2012]. Thus, studying persons with CIS offers a unique opportunity to understand the "first steps" of the pathophysiological mechanisms leading to MS.

By analogy with other neurodegenerative diseases [Maruszak and Thuret, 2014; de Flores et al., 2015], we hypothesize here that hippocampal degeneration in persons with CIS and early MS is not uniform and that pathological alterations will spread from one hippocampal subfield to the others in a process leading to diffuse hippocampal atrophy. To test this hypothesis, we measured the volumes of five distinct hippocampal subfields longitudinally, using advanced 3T MRI-based automatic segmentation techniques, and analysed the dynamics of atrophy of these subfields together with their clinical and neuropsychological correlates.

2. Methods

Participants

Fifty-six persons with CIS (PwCIS) were prospectively enrolled between 2 to 6 months after an initial clinical event compatible with a demyelinating inflammatory syndrome: a monofocal and monophasic neurological symptom that can be related to an optic nerve, spinal cord, brainstem, cerebral hemisphere or cerebellum lesion [Miller et al., 2012]. Patients were assessed by neuropsychological testing and MRI at baseline and at 1-year follow up. At baseline, at least two clinically silent lesions with a minimum diameter of 3mm were required for inclusion. One of these lesions had to be cerebral (ovoid or periventricular), while the other could be located in the spine or brain. None of the patients were treated with disease-modifying therapy at inclusion. Contraindications to MRI, the presence of other neurological, psychiatric or systemic diseases, steroid treatment within one month, starting or stopping antidepressants or anxiolytic treatments within 2 months of MRI and neuropsychological examination, were considered as exclusion criteria. During the follow-up period of one year, the diagnosis of multiple sclerosis was confirmed (or not) by the treating physician according to the 2010 McDonald criteria [Polman et al., 2011].

Fifty-five healthy controls (HC), free of neurological, psychiatric, or systemic diseases, and drug or alcohol abuse, were also included. They were tightly matched for age, gender and educational level to PwCIS, to calculate cognitive z-scores both at baseline and one year after (see below). Among these 55 controls, a subgroup of 38 HC (still matched with the CIS group, see Table 1) underwent MRI at baseline but they were not re-scanned at year 1.

All subjects were prospectively enrolled from 2012 to 2015 at our MS centre. Written

informed consent was obtained prior to participation. This study was approved by the local institutional ethics review board and registered in Clinicaltrial.gov (NCT01865357).

Neuropsychological testing

In order to assess hippocampal functions, PwCIS and HC performed the Selective Reminding Test (SRT) for episodic verbal memory performance and the Brief Visuospatial Memory Test (BVMT-R) to test episodic visuospatial memory performance. Each PwCIS was compared with the HC group at the appropriate time point to calculate a z-score for each test at each time point. To take into account practice effects, the scores of PwCIS at baseline were compared with the mean score of the HC group obtained at baseline, while the scores of PwCIS at 1 year were compared with the mean score of the HC group obtained during their second session of neuropsychological testing at 1 year. The z-scores of each SRT and BVMT-R subtest were averaged in order to calculate one composite verbal memory score and one composite visuospatial memory score. Lower z-scores indicate lower performance. A patient was considered impaired in a given cognitive domain if his/her score was below the fifth percentile (*i.e.* z-score < -1.64).

MRI acquisition and analyses

Participants were scanned on a 3T MRI system at our MS centre (either Philips Achieva or GE Medical Systems Discovery MR 750w). Thirteen patients (out of 46, *i.e.* 28%) were not scanned on the same machine at baseline and after one year (Philips Achieva at baseline and GE Discovery after 1 year). The imaging protocol was harmonized between magnets and included the same 3D gradient-echo T1-weighted sequence (TR/TE/TI/flip

angle=8.2ms/3.5ms/982ms/7°, resolution 1x1x1mm, 256mm FOV) and a 2D axial Fluid Attenuated Inversion Recovery (FLAIR) sequence (TR/TE/TI=11000ms/140ms/2800ms, resolution 1x1.1x3mm, 230mm FOV). Preliminary analyses (not shown) using the type of scanner as a covariate did not show any effect of the magnet on volumetric analyses.

Lesion load was determined by the lesion growth algorithm as implemented in the Lesion Segmentation Tool (LST) version 2.0.15 (http://www.applied-statistics.de/lst.html) in Statistical Parametric Mapping (SPM12) [Schmidt et al., 2012]. To do this, T1 images were co-registered with FLAIR images to calculate lesion belief maps, thresholded with the same parameters for each patient (kappa=0.3). Binary maps of lesions were reviewed and corrected manually by two blinded experts (MR engineer and neurologist), using 3D Slicer 4.4.0 (www.slicer.org).

For the volumetric analyses of brain structures and hippocampal subfields, T1-weighted images were processed using the volBrain system (http://volbrain.upv.es) [Manjón and Coupé, 2016]. After denoising with an adaptive non-local mean filter [Manjón et al., 2010], images were affine-registered in the Montreal Neurological Institute (MNI) space using ANTS software [Avants et al., 2011], corrected for image inhomogeneities using N4 [Tustison et al., 2010] and finally intensity-normalized [Nyúl and Udupa, 1999]. Then, the hippocampal subfields were segmented based on a multi-atlas framework combining nonlinear registration and patch-based label fusion [Romero et al., 2016; Romero et al., 2017]. This method uses a training library composed of 5 high resolution T1-weighted images labelled manually according to the protocol proposed by Winterburn and colleagues [Winterburn et al., 2013] which is one of the rare freely available atlases that specifically separate CA4/DG from CA2/3 on the one hand and CA1 neuritic and pyramidal layers on the other hand [Yushkevich et al., 2015]. The 3D-T1-weighted images of the subjects considered in this study ($1x1x1mm^3$) were up-sampled to the image resolution of the training library

(0.5x0.5x0.5mm^3) using the local adaptive super-resolution (LASR) method [Coupé et al., 2013]. The method finally provided automatic segmentation of hippocampal subfields gathered into 5 labels: Subiculum, CA1-SP (stratum pyramidale), CA1-SRLM (stratum radiatum-lacunosum-moleculare), CA2/3 and CA4/dentate gyrus (Fig. 1), allowing us to test our *a priori* hypotheses regarding the selective vulnerability of the dentate gyrus or CA1, as suggested in the literature from animal, neuropsychological (using pattern separation tasks) and MRI studies [Planche et al., 2017b; Planche et al., 2017c; Rocca et al., 2015; Sicotte et al., 2008]. In our previous paper, the hippocampal subfield segmentation accuracy using T1-weighted has been estimated to be 62% for the Winterburn protocol in terms of average DICE coefficient. Moreover, the whole hippocampus segmentation accuracy has been estimated to 88% in term of DICE coefficient. Finally, it has been shown that super-resolution enables to obtain an accuracy close the one obtained when using high resolution T1 [Romero et al., 2017]. Every up-sampled image and every subfield label were quality-controlled and manually corrected by a blinded neurologist if needed (in the case of inappropriate inclusion of para-hippocampal T1-hypointense lesions (Suppl. Fig. 1), choroidal plexus and/or CSF "pockets", using 3D Slicer 4.4.0 (www.slicer.org)). To control for variations in head size, the volumes of hippocampal subfields were normalized using the intracranial cavity volume of each subject [Manjón et al., 2014]. Normalized brain volume (NBV) was also calculated as the sum of cerebral white and grey matters, divided by the intracranial cavity volume of each subject.

Statistical Analyses

Statistical analyses were performed with Prism software 6 (Graphpad) and XLstats 19.4 (Addinsoft). The distribution of all continuous data was tested with the Shapiro-Wilk normality test. We first compared clinical, neuropsychological and imaging characteristics

between HC and PwCIS at baseline by using Fisher's exact tests for categorical variables, and unpaired t-tests or Mann-Whitney tests for ordinal variables. The comparisons of baseline and 1-year characteristics of PwCIS were done with paired t-tests or Wilcoxon tests, as appropriate.

To compare the volumes of the 5 hippocampal subfields between groups, we first performed an analysis of variance, followed by a Sidak multiple comparisons test. Cohen's d was used to measure the effect size of atrophy between patients and HC whereas annualized rate of atrophy was used to compare PwCIS at year 1 and baseline.

Then, because the decreases in subfield volumes were consistent between right and left hippocampi, further statistical analyses were performed on the sum of right and left subfield volumes to avoid multiple comparisons. Relationships between neuropsychological scores, demographic, clinical and imaging variables were assessed using correlation coefficients (Pearson or Spearman according to statistical distribution). The associations were further tested in multivariate context. To this end, *(i)* hippocampal subfields volumes at year 1, *(ii)* MS diagnosis after 1-year follow-up and *(iii)* memory performance (dependent variables) were predicted with hierarchical regression models, including two hierarchical blocks. In the first block, relevant demographical, clinical and general MRI features known as nuisance variables were systematically forced into the model. In the second block, the volumes of hippocampal subfields were added to the variables of the first block. The predictive power of the two blocks was compared by using the Akaike information criterion (AIC). A linear regression model was used whenever possible while logistic regression was seen as the appropriate alternative for categorical/binary outcome variables. All tests were two-tailed, with a global type I error set at $\alpha=0.05$.

Results

Demographic, clinical and general MRI features of participants

A total of 56 PwCIS and 55 HC were included. At baseline, all PwCIS and HC were tested with the neuropsychological battery while all PwCIS but only a subgroup 38 HCs were assessed with MRI. At year 1, because 10 patients were lost to follow-up, 46 PwCIS were re-tested with the same neuropsychological battery and re-scanned with the same imaging protocol. All the 55 HCs were re-tested with the same neuropsychological battery but they were not re-scanned at year 1.

The CIS and HC groups were comparable for age, sex and educational level (Table 1). In this cohort of patients, after one year, 65.2% of PwCIS were diagnosed with MS according to the 2010 McDonald criteria.

In PwCIS, there was no significant difference between baseline and 1-year follow-up regarding disability (Expanded Disability Status Scale, EDSS) and T2-lesion load. Neuropsychological testing was also rather stable between baseline and 1-year follow-up, except for the episodic visuospatial memory score that had even slightly increased (p=0.02) (Table 1). Normalized brain volume (NBV) significantly decreased during this period (-1.4%, p=0.012).

Dynamics of regional hippocampal vulnerability

At baseline, hippocampal volumes were significantly lower in PwCIS compared to controls only in the CA4/dentate gyrus subfield (Fig. 2). This was consistently true for the left (-6.5%, d=0.53, p<0.05) and for the right hippocampus (-7.7%, d=0.54, p<0.01) and when both sides were pooled together (-7.2%, d=0.58, p<0.01). In PwCIS, this atrophy of CA4/dentate gyrus was not correlated with age, disability or T2 lesion-load at baseline.

Follow-up data after one year compared to baseline measures showed that the normalized volumes of CA4/dentate gyrus (-6.4%, p<0.001), CA1-SP (-5,6%, p<0.01) and CA1-SRLM (-6,2%, p<0.05) significantly decreased in both sides. No significant atrophy was found in the subiculum or CA2/3 subfields (Fig. 3).

As the atrophy of CA1 subfield chronologically succeeded the atrophy of CA4/dentate gyrus, this suggests that the same pathophysiological process spreads from CA4/dentate gyrus to CA1 in individual patients. To test this hypothesis, we designed a hierarchical linear regression model to test how CA1-SP, CA1–SRLM and whole hippocampus volumes at year 1 (dependent variables) can be predicted by the volume of CA4/dentate gyrus at baseline (while first taking into account confounders such as age, T2 lesion-load and NBV in the model). We found that CA4/dentate gyrus at baseline improved the statistical prediction of CA1 volumes at year 1 from R^2=0.19 (when considering usual factors such as age, T2 lesions and NBV) to R^2=0.44 ($AIC_{block2} < AIC_{block1}$). It also predicted the whole hippocampal volume one year afterwards independently of age, T2 lesions or NBV (Table 2). CA4/DG remained a significant and independent correlate of CA1 and whole hippocampal volumes at year 1, although other hippocampal subfields (subiculum and CA2/3) were introduced in the model (ß=0.34, p=0.018 for CA1-SP and ß=0.39, p<0.001 for the whole hippocampus, respectively). Altogether, a smaller focal volume at baseline predicted smaller global volumes at year 1, which points to a pathological continuum starting within CA4/dentate gyrus and spreading progressively and more globally to CA1.

Relationship between the atrophy of hippocampal subfields and clinical outcomes

In order to study the link between the early vulnerability of CA4/dentate gyrus and the pathophysiological process specific to MS, we first investigated whether CA4/dentate gyrus volume at baseline would be able to predict MS diagnosis at year 1. Using univariate analyses, we found that both T2-lesion load and CA4/dentate gyrus volume were significantly associated MS diagnosis after 1-year follow-up (p=0.002 and p=0.014, respectively). A multiple logistic regression model showed that the volume of CA4/dentate gyrus at baseline was the only factor independently associated with future MS diagnosis (ß=0.57, p=0.025 and R^2=0.28, p=0.016) while age, gender, EDSS, T2-lesion load and NBV were not predictive.

Finally, we investigated whether early hippocampal regional vulnerability had a clinical impact on episodic memory performance. The results of univariate correlations and regression models between memory scores and demographic, clinical and imaging data at baseline and year 1 are presented in Table 3. According to multivariate analyses, no model was able to explain memory performance at baseline. The volume of CA1-SP and the educational level of patients were independent predictors of the episodic verbal memory composite score at year 1 (ß=0.87, p=0.042 and ß=0.51, p=0.031, respectively).

Discussion

We demonstrated in this study that the CA4/dentate gyrus subfield of the hippocampus is the first subfield to be atrophied across the course of MS, at the stage of CIS. This pattern of regional hippocampal atrophy worsens during the first year of disease evolution and spreads within CA1 (both in the cell bodies layer CA1-SP and the neuritic layers CA1-SRLM). CA4/dentate gyrus volume at baseline was associated with diagnosis of MS one year afterwards. Whereas isolated CA4/dentate gyrus atrophy at the stage of CIS failed to correlate with memory scores, it predicted the extension of the pathological process within CA1 one year later, which was in turn correlated with episodic verbal memory performance, independently of usual confounders.

Our main finding of a "natural history" of hippocampal subfield degeneration in MS, from dentate gyrus to CA1, is supported by anatomical and functional studies in both human and animal models of the disease. First, we previously reported that pattern separation performance - a cognitive task critically dependant on dentate gyrus function [Bakker et al., 2008] - was decreased in patients with CIS and early MS, when conventional visuospatial episodic memory tests (BVMT-R) were not yet altered, suggesting an early and isolated dentate gyrus dysfunction during the course of the disease [Planche et al., 2017c]. Such functional alterations suggested by the pattern separation task are therefore consolidated by the anatomical alterations observed in the present MRI study. Second, our findings are also supported by a previous work showing that dentate gyrus structure and function are selectively disrupted by microglial activation at the early stage of experimental autoimmune encephalomyelitis (EAE, the animal model of MS) [Planche et al., 2017b]. The independent association we found here between CA4/dentate gyrus volume at the stage of CIS and the diagnosis of MS one year after CIS also suggests this link between dentate gyrus damage and the early diffuse pathophysiological process specific to MS. Third, the vulnerability of the

dentate gyrus, prior to other hippocampal subfields at the early stage of MS, could be explained by its particular anatomical location. Indeed, it is adjacent to cerebrospinal fluid (CSF) spaces (third ventricle in rodents and choroidal fissure in humans) where cytokines and immune cells preferentially penetrate the hippocampus, as suggested experimentally in EAE [Habbas et al., 2015]. We postulate that the hierarchical vulnerability of hippocampal subfields in MS might be better explained by their anatomical contiguity rather than by a network-dependent disposition, as in Alzheimer's disease for instance [Kerchner et al., 2013]. A gradient of infiltrating immune cells and cytokines would diffuse progressively from the CSF to the dentate gyrus, then to CA1, and probably to the whole medial temporal lobe. In this model, the progression of the disease from the dentate gyrus to CA1 might be slowed down by the presence of the vestigial intrahippocampal sulcus, potentially explaining the delay between dentate gyrus and CA1 atrophy reported in this study. Additional experiments will be needed to test these mechanistic hypotheses.

From the anatomopathological point of view, our study also highlights the striking vulnerability of the hippocampus to neurodegeneration in the context of neuroinflammation. Indeed, the annualized rate of atrophy during the first year of the disease's evolution ranged from -5.6% to -6.4%, respectively for CA1 and CA4/dentate gyrus, whereas it was 'only' -1.4% for the normalized brain volume in our population of PwCIS (which was in the upper range of what was usually observed in the literature on CIS and relapsing MS, *i.e.* from -0.5% to -1.35% [Pérez-Miralles et al., 2013; De Stefano et al., 2014]). This selective and disproportionate hippocampal volume loss, in excess to global brain atrophy, has already been observed in a seminal cross-sectional study on patients with relapsing and progressive MS [Sicotte et al., 2008]. The annualized rate of hippocampal atrophy we report here (-5.9%) is even in the upper range of what has been reported for patients with Alzheimer's disease or mild cognitive impairment (-3.5% to -6%/year) [Jack et al., 2000; Wang et al., 2003; Du et

al., 2004] and far beyond what has been reported for physiological aging (-0.8% to -2.3%/year) [Jack et al., 2011].

Besides these anatomical considerations, we also questioned the link between the early regional vulnerability of the hippocampus and memory impairment in MS. On the one hand, the CA4/dentate gyrus atrophy observed at baseline was not correlated with episodic memory performance in our cohort. Although we have to take into account that the memory abilities of the PwCIS included in this study were not severely affected (regarding the median z-scores and the percentage of impaired patients), we postulate that CA4/dentate gyrus atrophy at the stage of CIS is "not enough" to explain the memory decline observed in "global" episodic memory tests such as the SRT or the BVMT-R. Perhaps more specific tests such as the behavioural pattern separation task [Stark et al., 2013] would have allowed us to pinpoint such a subtle memory decline related to CA4/dentate gyrus damage [Planche et al., 2017c] and future studies should address this point. On the other hand, we found that CA1 atrophy explained part of the "global" episodic verbal memory decline one year after inclusion, when diagnosis of MS was finally observed in 65.2% of the patients. This suggests that CA1 atrophy is the best anatomical correlate of memory performance in MS, as previously described in cross-sectional studies including patients with relapsing and progressive MS [Sicotte et al., 2008; Longoni et al., 2015].

A recent cross-sectional study found an "expansion" of the dentate gyrus during MS [Rocca et al., 2015]. The divergences between our findings and this previous work may be attributed to various points. Indeed, contrary to our work, this study investigated patients at a later stage of the disease, with relapsing and progressive MS, and it used a surface-based mesh modelling technique to study the shape of the hippocampus [Thompson et al., 2004]. Using this technique, the authors found an outward displacement of the supero-medial hippocampal surface and concluded on a larger radial distance of the dentate gyrus in patients with MS.

However, it should be borne in mind that when using such a method, measuring external surface modifications does not enable the direct characterization of the inner alterations of a particular subfield. It is not clear how the atrophy of the deepest regions of the hippocampus (such as the dentate gyrus, which is curled inside the Cornu Ammonis) would impact the outer surface of the structure. For instance, the expansion of CSF pockets due to atrophy within the hippocampal fissure/sulcus might result in tissue "expansion" on the supero-medial side of the hippocampus despite there being no real dentate gyrus "hypertrophy". We also hypothesized that a shift of rotation of the hippocampus due to atrophy would induce an outward displacement of part of the surface, introducing contradictory results. Thus, radial mapping provides valuable information on hippocampal surface change (*i.e.* CA1 and the subiculum) but should be interpreted with caution for inner structures such as the dentate gyrus [La Joie et al., 2010]. The limits of these surface-based modelling strategies to assess hippocampal subfield anatomy have been discussed extensively in the field of Alzheimer's disease and aging [de Flores et al., 2015; Morra et al., 2009], even by the authors who pioneered the method [Thompson et al., 2004; Frisoni et al., 2008]. Therefore, proper volumetric analyses with manual or automatic segmentation are now considered more relevant than radial mapping to investigate hippocampal regional vulnerability, although they have their own limitations and require protocol harmonization to clearly define subfield boundaries [Wisse et al., 2017]. For instance, we acknowledge that the Winterburn protocol we used here mainly delineates CA2/3 in its dorsal portion to increase segmentation reliability, although it can lead to volume underestimations. Therefore, our results might have differed by using other definitions of the hippocampal subfields boundaries. From the technical point of view, we also acknowledge that we only used T1-weighted images to label hippocampal subfields, whereas both T1 and T2-weighted images are often preferred to delineate internal boundaries, especially for very thin layers such as CA1-SRLM. However

pooling CA1-SRLM with the bigger CA1-SP wouldn't have changed our main conclusions. Furthermore, we have recently validated that the single use of T1-weighted images up-sampled with local adaptive super-resolution leads to reliable hippocampal subfield labeling, compared to the combination of T1 and T2-weighted images [Romero et al., 2017].

The main limitation of our study is the lack of MRI follow-up for our healthy control group to clearly disentangle the contribution of time-dependant *versus* disease-dependant processes in our longitudinal measures of atrophy in the CIS group. However, our results on the dynamics of progressive hippocampal subfield atrophy are likely related to the disease process because they are specific (*i.e.* CA4/dentate gyrus and CA1 but not CA2/3 and the subiculum) and because the annualized rate of hippocampal atrophy measured (-5.9%/year) is clearly above what can be observed on average in the healthy population (-0.4%/year in people less than 55 years old) [Fraser et al., 2015]. Another limitation is the short follow-up period (1-year), which was nonetheless long enough to capture the sequential progression of hippocampal subfield atrophy. We also acknowledge that we did not assess the potential microstructural damage that underlies or precedes hippocampal regional atrophy, with sequences such as diffusion-tensor imaging or magnetization transfer MRI, but these techniques are difficult to implement at the spatial resolution required to study hippocampal subfields. The final limitation was that, although no area of T2-hypersignal or T1-black hole was clearly detected within the hippocampus on our conventional sequences, we did not assess potential subtle demyelinating hippocampal lesions with specific double inversion recovery sequences.

Conclusion

We demonstrated that CA4/dentate gyrus is the first subfield of the hippocampus to be atrophied during the course of MS, from the stage of CIS. This regional pattern of hippocampal atrophy rapidly spread to CA1. This dynamic vulnerability is associated with future diagnosis of MS and contributes to hippocampal-dependant memory performance.
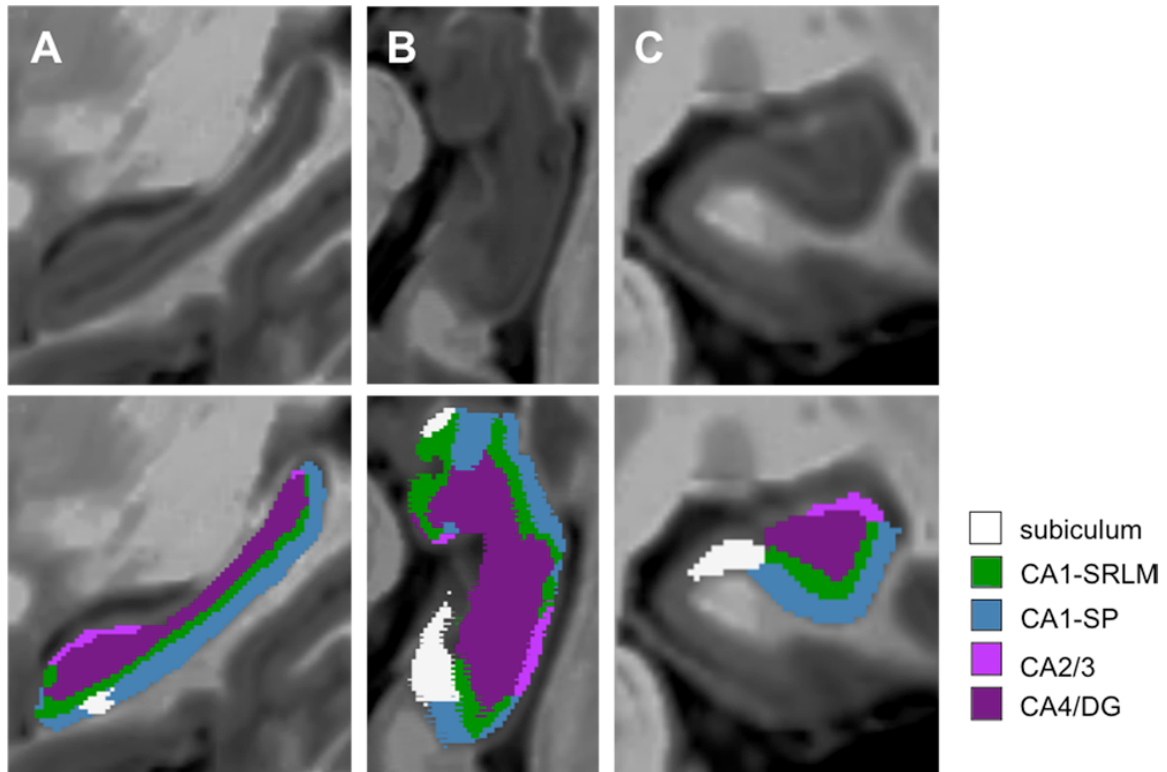
Figure 1: Segmentation of the five hippocampal subfields.

Super-resolution T1-weighted images ($0.5 \times 0.5 \times 0.5 \text{mm}^3$) centred on the left hippocampus of a patient with clinically isolated syndrome (PwCIS) in the sagittal plane (A), in an oblique axial cut parallel to the plane of the hippocampus (B) and in the coronal plane (C). Five hippocampal subfields were automatically segmented (and manually corrected if needed) according to the atlas of Winterburn *et al*.: the subiculum, the stratum pyramidale of CA1 (CA1-SP), the stratum-lacunosum-moleculare of CA1 (CA1-SRLM), CA2/3 and CA/4dentate gyrus (CA4/DG).
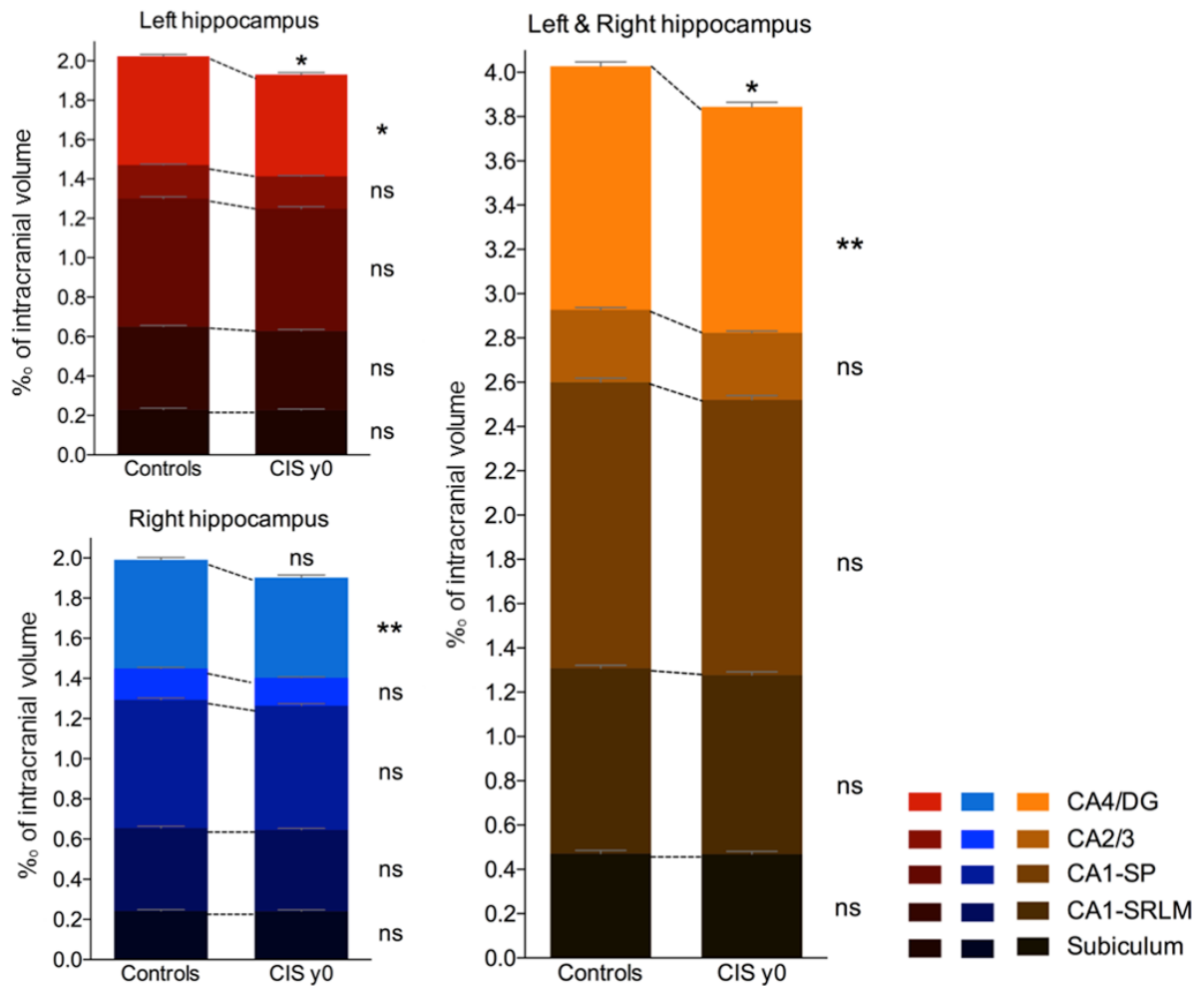
Figure 2: Comparison of the normalized volumes of hippocampal subfields between healthy controls and persons with clinically isolated syndrome (CIS) at baseline (y0).

Histograms represent the cumulative volumes of all the left hippocampal subfields (in red), of all the right hippocampal subfields (in blue) and of all right&left hippocampal subfields (in orange). The colour gradient represents individual hippocampal subfields. ns = non-significant, $*p<0.05$, $**p<0.01$ (corrected for multiple comparisons).
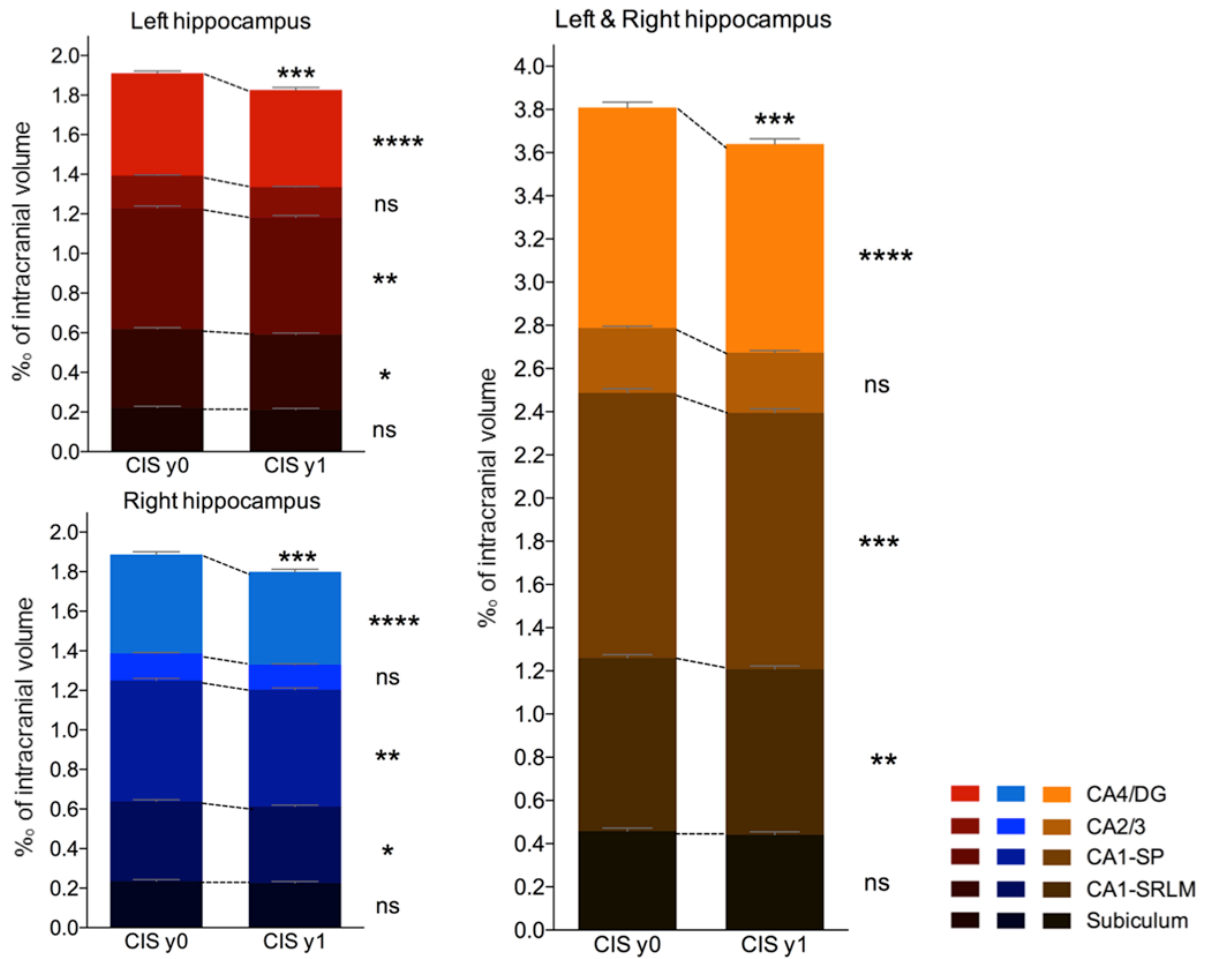
Figure 3: Comparison of the normalized volumes of hippocampal subfields between persons with clinically isolated syndrome (CIS) at baseline (y0) and 1-year follow-up (y1).

The histograms represent the cumulative volumes of all the left hippocampal subfields (in red), of all the right hippocampal subfields (in blue) and of all right&left hippocampal subfields (in orange). The colour gradient represents individual hippocampal subfields. ns = non-significant, *p<0.05, **p<0.01, ***p<0.001, ****p<0.0001 (corrected for multiple comparisons).

	Controls with MRI (n=38)	CIS baseline (n=56)	CIS 1-year (n=46)	*p-value*
Demographic and clinical features				
Mean age, years [SD]	36.6 [10.7]	36.5 [11.2]	-	0.94
Sex ratio (F/M)	26/12	46/10	-	0.14
Education level, (High/Low§)	27/11	39/17	-	0.88
Median EDSS score [range]	-	1.0 [1.0 to 6.0]	1.0 [1.0 to 6.0]	0.63
Conversion to MS	-	-	30/46 (65.2%)	-
Neuropsychological features				
Median verbal memory z-score [range]		0.10 [-4.9 to 1.0]	-0.13 [-3.7 to 1.2]	0.91
{% impaired}		{7.4%}	{10.7%}	
Median visuospatial memory z-score [range]		-0.20 [-5.2 to 0.82]	0.10 [-3.5 to 1.0]	0.02
{% impaired}		{17.9%}	{6.5%}	
Imaging features				
Median T2 lesion volume, mL [range]	-	0.73 [0.02-63.12]	1.08 [0.06-67.74]	0.67
Mean normalized brain volume, % [SD]	86.4 [3.2]	85.1 [3.9]	83.9 [4.1]	0.21[#]/0.012[†]

Table 1: Clinical, neuropsychological and general MRI features of the studied populations. CIS = Clinically Isolated Syndrome; EDSS = Expanded Disability Status Scale; MS: Multiple Sclerosis; SD = Standard Deviation. § Education level was considered as high or low according to French baccalaureate (equivalent to A-level). # Controls vs CIS baseline. † CIS baseline vs CIS 1-year.

1 year volume		Explanatory variables (at baseline)	Univariate analysis (r)	Multivriate analysis (ß)	Adjusted multivariate model (R²)
CA1-SP	*Block 1*	Age	-0.16	ns	0.19*
		T2LL	-0.21	ns	
		NBV	0.44**	0.47*	
	Block 2	Age	-0.16	ns	0.44***#
		T2LL	-0.21	ns	
		NBV	0.44**	ns	
		CA4/DG	0.63***	0.40***	
CA1-SRLM	*Block 1*	Age	-0.06	ns	0.27**
		T2LL	-0.16	ns	
		NBV	0.48***	0.64***	
	Block 2	Age	-0.06	ns	0.47***#
		T2LL	-0.16	ns	
		NBV	0.48***	0.40*	
		CA4/DG	0.62***	0.47***	
Hippocampus	*Block 1*	Age	-0.16	ns	0.32**
		T2LL	-0.26	ns	
		NBV	0.56***	0.65***	
	Block 2	Age	-0.16	ns	0.61***#
		T2LL	-0.26	ns	
		NBV	0.56***	0.37*	
		CA4/DG	0.71***	0.58***	

Table 2: Univariate correlations and hierarchical linear regression models between volumes of CA1 subfields or whole hippocampal volume at year 1 (dependent variables) and volume of CA4/dentate gyrus at baseline. Age, T2LL and NBV were entered into an initial model (block 1) as nuisance variables. CA1-SP = CA1-stratum pyramidale, CA1-SRLM = CA1-stratum radiatum-lacunosum-moleculare, CA4/DG = CA4/dentate gyrus, NBV = Normalized Brain Volume, T2LL = T2 Lesion-Load. ns = non-significant, *p<0.05, **p<0.01, ***p<0.001. # $AIC_{block2} < AIC_{block1}$.

		Explanatory variables	Univariate analysis (r)	Multivariate analysis (ß)	Adjusted multivariate model (R^2)
Baseline					
Episodic verbal memory	*Block 1*	Age	-0.04	ns	ns
		T2LL	-0.20	ns	
		NBV	0.12	ns	
		Education level	0.32*	0.38*	
	Block 2[§]	-	-	-	-
Episodic spatial memory	*Block 1*	Age	-0.18	ns	ns
		T2LL	-0.18	ns	
		NBV	0.17	ns	
		Education level	0.32*	ns	
	Block 2[§]	-	-	-	-
1 year					
Episodic verbal memory	*Block 1*	Age	-0.15	ns	ns
		T2LL	-0.14	ns	
		NBV	0.17	ns	
		Education level	0.24	ns	
	Block 2	Age	-0.15	ns	0.26*
		T2LL	-0.14	ns	
		NBV	0.17	ns	
		Education level	0.24	0.51*	
		CA1-SP	0.30*	0.87*	
		CA1-SRLM	0.24	ns	
Episodic spatial memory	*Block 1*	Age	-0.35*	ns	ns
		T2LL	-0.17	ns	
		NBV	-0.03	ns	
		Education level	0.14	ns	
	Block 2[§]	-	-	-	-

Table 3: Univariate correlations and hierarchical regression models between memory composite scores at baseline or after 1-year follow-up (dependent variables) and demographical, clinical and MRI features. Age, T2LL, NBV and educational level were entered into an initial model (block 1) as nuisance variables. Covariables related to hippocampal subfields were added in a second model (block 2) according to univariate correlations (p-value <0.2) to predict memory scores. CA1-SP = CA1-stratum pyramidale, CA1-SRLM = CA1-stratum radiatum-lacunosum-moleculare, T2LL = T2 Lesion-Load. NBV = Normalized Brain Volume. ns = non-significant, *p<0.05. [§]: Block 2 was equivalent to Block 1 because no correlation (p<0.2) was found between the volume of any hippocampal subfields and the memory score.

References

Avants BB, Tustison NJ, Song G, Cook PA, Klein A, Gee JC (2011): A reproducible evaluation of ANTs similarity metric performance in brain image registration. NeuroImage 54:2033–2044.

Bakker A, Kirwan CB, Miller M, Stark CEL (2008): Pattern separation in the human hippocampal CA3 and dentate gyrus. Science 319:1640–1642.

Coupé P, Manjón JV, Chamberland M, Descoteaux M, Hiba B (2013): Collaborative patch-based super-resolution for diffusion-weighted images. NeuroImage 83:245–261.

De Stefano N, Airas L, Grigoriadis N, Mattle HP, O'Riordan J, Oreja-Guevara C, Sellebjerg F, Stankoff B, Walczak A, Wiendl H, Kieseier BC (2014): Clinical relevance of brain volume measures in multiple sclerosis. CNS Drugs 28:147–156.

Du AT, Schuff N, Kramer JH, Ganzer S, Zhu XP, Jagust WJ, Miller BL, Reed BR, Mungas D, Yaffe K, Chui HC, Weiner MW (2004): Higher atrophy rate of entorhinal cortex than hippocampus in AD. Neurology 62:422–427.

Dutta R, Chang A, Doud MK, Kidd GJ, Ribaudo MV, Young EA, Fox RJ, Staugaitis SM, Trapp BD (2011): Demyelination causes synaptic alterations in hippocampi from multiple sclerosis patients. Ann Neurol 69:445–454.

de Flores R, La Joie R, Chételat G (2015): Structural imaging of hippocampal subfields in healthy aging and Alzheimer's disease. Neuroscience 309:29–50.

Fraser MA, Shaw ME, Cherbuin N (2015): A systematic review and meta-analysis of longitudinal hippocampal atrophy in healthy human ageing. NeuroImage 112:364–374.

Frisoni GB, Ganzola R, Canu E, Rüb U, Pizzini FB, Alessandrini F, Zoccatelli G, Beltramello A, Caltagirone C, Thompson PM (2008): Mapping local hippocampal changes in Alzheimer's disease and normal ageing with MRI at 3 Tesla. Brain 131:3266–3276.

Gold SM, Kern KC, O'Connor M-F, Montag MJ, Kim A, Yoo YS, Giesser BS, Sicotte NL (2010): Smaller cornu ammonis 2-3/dentate gyrus volumes and elevated cortisol in multiple sclerosis patients with depressive symptoms. Biol Psychiatry 68:553–559.

Habbas S, Santello M, Becker D, Stubbe H, Zappia G, Liaudet N, Klaus FR, Kollias G, Fontana A, Pryce CR, Suter T, Volterra A (2015): Neuroinflammatory TNFα Impairs Memory via Astrocyte Signaling. Cell 163:1730–1741.

Hulst HE, Schoonheim MM, Van Geest Q, Uitdehaag BMJ, Barkhof F, Geurts JJG (2015): Memory impairment in multiple sclerosis: Relevance of hippocampal activation and hippocampal connectivity. Mult Scler 21:1705–1712.

Jack CR, Petersen RC, Xu Y, O'Brien PC, Smith GE, Ivnik RJ, Boeve BF, Tangalos EG, Kokmen E (2000): Rates of hippocampal atrophy correlate with change in clinical status in aging and AD. Neurology 55:484–489.

Jack CR, Barkhof F, Bernstein MA, Cantillon M, Cole PE, Decarli C, Dubois B, Duchesne S, Fox NC, Frisoni GB, Hampel H, Hill DLG, Johnson K, Mangin J-F, Scheltens P, Schwarz AJ, Sperling R, Suhy J, Thompson PM, Weiner M, Foster NL (2011): Steps to standardization and validation of hippocampal volumetry as a biomarker in clinical trials and diagnostic criterion for Alzheimer's disease. Alzheimers Dement 7:474–485.e4.

Kerchner GA, Bernstein JD, Fenesy MC, Deutsch GK, Saranathan M, Zeineh MM, Rutt BK (2013): Shared vulnerability of two synaptically-connected medial temporal lobe areas to age and cognitive decline: a seven tesla magnetic resonance imaging study. J Neurosci 33:16666–16672.

La Joie R, Fouquet M, Mézenge F, Landeau B, Villain N, Mevel K, Pélerin A, Eustache F, Desgranges B, Chételat G (2010): Differential effect of age on hippocampal subfields assessed using a new high-resolution 3T MR sequence. NeuroImage 53:506–514.

Longoni G, Rocca MA, Pagani E, Riccitelli GC, Colombo B, Rodegher M, Falini A, Comi G, Filippi M (2015): Deficits in memory and visuospatial learning correlate with regional hippocampal atrophy in MS. Brain Struct Funct 220:435–444.

Manjón JV, Coupé P (2016): volBrain: An Online MRI Brain Volumetry System. Front Neuroinformatics 10:30.

Manjón JV, Coupé P, Martí-Bonmatí L, Collins DL, Robles M (2010): Adaptive non-local means denoising of MR images with spatially varying noise levels. J Magn Reson Imaging JMRI 31:192–203.

Manjón JV, Eskildsen SF, Coupé P, Romero JE, Collins DL, Robles M (2014): Nonlocal intracranial cavity extraction. Int J Biomed Imaging 2014:820205.

Maruszak A, Thuret S (2014): Why looking at the whole hippocampus is not enough-a critical role for anteroposterior axis, subfield and activation analyses to enhance predictive value of hippocampal changes for Alzheimer's disease diagnosis. Front Cell Neurosci 8:95.

Miller DH, Chard DT, Ciccarelli O (2012): Clinically isolated syndromes. Lancet Neurol 11:157–169.

Morra JH, Tu Z, Apostolova LG, Green AE, Avedissian C, Madsen SK, Parikshak N, Hua X, Toga AW, Jack CR, Schuff N, Weiner MW, Thompson PM, Alzheimer's Disease Neuroimaging Initiative (2009): Automated 3D mapping of hippocampal atrophy and its clinical correlates in 400 subjects with Alzheimer's disease, mild cognitive impairment, and elderly controls. Hum Brain Mapp 30:2766–2788.

Nyúl LG, Udupa JK (1999): On standardizing the MR image intensity scale. Magn Reson Med 42:1072–1081.

Papadopoulos D, Dukes S, Patel R, Nicholas R, Vora A, Reynolds R (2009): Substantial archaeocortical atrophy and neuronal loss in multiple sclerosis. Brain Pathol 19:238–253.

Pérez-Miralles F, Sastre-Garriga J, Tintoré M, Arrambide G, Nos C, Perkal H, Río J, Edo MC, Horga A, Castilló J, Auger C, Huerga E, Rovira A, Montalban X (2013): Clinical impact of early brain atrophy in clinically isolated syndromes. Mult Scler 19:1878–1886.

Planche V, Ruet A, Coupé P, Lamargue-Hamel D, Deloire M, Pereira B, Manjon JV, Munsch F, Moscufo N, Meier DS, Guttmann CR, Dousset V, Brochet B, Tourdias T (2017a): Hippocampal microstructural damage correlates with memory impairment in clinically isolated syndrome suggestive of multiple sclerosis. Mult Scler 23:1214–1224.

Planche V, Panatier A, Hiba B, Ducourneau E-G, Raffard G, Dubourdieu N, Maitre M, Lesté-Lasserre T, Brochet B, Dousset V, Desmedt A, Oliet SH, Tourdias T (2017b): Selective dentate gyrus disruption causes memory impairment at the early stage of experimental multiple sclerosis. Brain Behav Immun 60:240–254.

Planche V, Ruet A, Charré-Morin J, Deloire M, Brochet B, Tourdias T (2017c): Pattern separation performance is decreased in patients with early multiple sclerosis. Brain Behav

7(8):e00739.

Polman CH, Reingold SC, Banwell B, Clanet M, Cohen JA, Filippi M, Fujihara K, Havrdova E, Hutchinson M, Kappos L, Lublin FD, Montalban X, O'Connor P, Sandberg-Wollheim M, Thompson AJ, Waubant E, Weinshenker B, Wolinsky JS (2011): Diagnostic criteria for multiple sclerosis: 2010 revisions to the McDonald criteria. Ann Neurol 69:292–302.

Rocca MA, Longoni G, Pagani E, Boffa G, Colombo B, Rodegher M, Martino G, Falini A, Comi G, Filippi M (2015): In vivo evidence of hippocampal dentate gyrus expansion in multiple sclerosis. Hum Brain Mapp 36:4702–4713.

Romero JE, Coupe P, Manjón JV (2016): High Resolution Hippocampus Subfield Segmentation Using Multispectral Multiatlas Patch-Based Label Fusion. In: Patch-Based Techniques in Medical Imaging. Springer, Cham. Lecture Notes in Computer Science pp 117–124.

Romero JE, Coupé P, Manjón JV (2017): HIPS: A new hippocampus subfield segmentation method. NeuroImage 163:286–295.

Schmidt P, Gaser C, Arsic M, Buck D, Förschler A, Berthele A, Hoshi M, Ilg R, Schmid VJ, Zimmer C, Hemmer B, Mühlau M (2012): An automated tool for detection of FLAIR-hyperintense white-matter lesions in Multiple Sclerosis. NeuroImage 59:3774–3783.

Sicotte NL, Kern KC, Giesser BS, Arshanapalli A, Schultz A, Montag M, Wang H, Bookheimer SY (2008): Regional hippocampal atrophy in multiple sclerosis. Brain 131:1134–1141.

Small SA (2014): Isolating pathogenic mechanisms embedded within the hippocampal circuit through regional vulnerability. Neuron 84:32–39.

Stark SM, Yassa MA, Lacy JW, Stark CEL (2013): A task to assess behavioral pattern separation (BPS) in humans: Data from healthy aging and mild cognitive impairment. Neuropsychologia 51:2442–2449.

Thompson PM, Hayashi KM, De Zubicaray GI, Janke AL, Rose SE, Semple J, Hong MS, Herman DH, Gravano D, Doddrell DM, Toga AW (2004): Mapping hippocampal and ventricular change in Alzheimer disease. NeuroImage 22:1754–1766.

Tustison NJ, Avants BB, Cook PA, Zheng Y, Egan A, Yushkevich PA, Gee JC (2010):

N4ITK: improved N3 bias correction. IEEE Trans Med Imaging 29:1310–1320.

Wang L, Swank JS, Glick IE, Gado MH, Miller MI, Morris JC, Csernansky JG (2003): Changes in hippocampal volume and shape across time distinguish dementia of the Alzheimer type from healthy aging. NeuroImage 20:667–682.

West MJ, Coleman PD, Flood DG, Troncoso JC (1994): Differences in the pattern of hippocampal neuronal loss in normal ageing and Alzheimer's disease. Lancet 344:769–772.

Winterburn JL, Pruessner JC, Chavez S, Schira MM, Lobaugh NJ, Voineskos AN, Chakravarty MM (2013): A novel in vivo atlas of human hippocampal subfields using high-resolution 3 T magnetic resonance imaging. NeuroImage 74:254–265.

Wisse LEM, Daugherty AM, Olsen RK, Berron D, Carr VA, Stark CEL, Amaral RSC, Amunts K, Augustinack JC, Bender AR, Bernstein JD, Boccardi M, Bocchetta M, Burggren A, Chakravarty MM, Chupin M, Ekstrom A, de Flores R, Insausti R, Kanel P, Kedo O, Kennedy KM, Kerchner GA, LaRocque KF, Liu X, Maass A, Malykhin N, Mueller SG, Ofen N, Palombo DJ, Parekh MB, Pluta JB, Pruessner JC, Raz N, Rodrigue KM, Schoemaker D, Shafer AT, Steve TA, Suthana N, Wang L, Winterburn JL, Yassa MA, Yushkevich PA, la Joie R, Hippocampal Subfields Group (2017): A harmonized segmentation protocol for hippocampal and parahippocampal subregions: Why do we need one and what are the key goals? Hippocampus 27:3–11.

Yushkevich PA, Amaral RSC, Augustinack JC, Bender AR, Bernstein JD, Boccardi M, Bocchetta M, Burggren AC, Carr VA, Chakravarty MM, Chételat G, Daugherty AM, Davachi L, Ding S-L, Ekstrom A, Geerlings MI, Hassan A, Huang Y, Iglesias JE, La Joie R, Kerchner GA, LaRocque KF, Libby LA, Malykhin N, Mueller SG, Olsen RK, Palombo DJ, Parekh MB, Pluta JB, Preston AR, Pruessner JC, Ranganath C, Raz N, Schlichting ML, Schoemaker D, Singh S, Stark CEL, Suthana N, Tompary A, Turowski MM, Van Leemput K, Wagner AD, Wang L, Winterburn JL, Wisse LEM, Yassa MA, Zeineh MM, Hippocampal Subfields Group (HSG) (2015): Quantitative comparison of 21 protocols for labeling hippocampal subfields and parahippocampal subregions in in vivo MRI: towards a harmonized segmentation protocol. NeuroImage 111:526–541.